Biochemical Pharmacology 242 (2025) 117219

Contents lists available at ScienceDirect

Biochemical Pharmacology

journal homepage: www.elsevier.com/locate/biochempharm

Lysosomal TPC2 channel as a new target of chlorpromazine and clomipramine to induce protective autophagy in L-BMAA-induced neurodegeneration

Valentina Tedeschi [a], Raffaella Ciancio [a], Giorgia Magliocca [a], Emilia Esposito [a], Silvia Piccirillo [b], Valentina Rubino [c], Alessandra Preziuso [b], Tatiana Spadoni [b,d], Noemi Di Muraglia [a,e], Giuseppina Ruggiero [c], Anna Pannaccione [a], Agnese Secondo [b,*]

[a] Division of Pharmacology, Department of Neuroscience, Reproductive and Odontostomatological Sciences, School of Medicine, University of Naples "Federico II", Via S. Pansini 5, Naples 80131, Italy
[b] Department of Biomedical Sciences and Public Health, School of Medicine, University "Politecnica delle Marche", Via Tronto 10/A, Ancona 60126, Italy
[c] Department of Translational Medical Sciences, University of Naples "Federico II", Via S. Pansini 5, Naples 80131, Italy
[d] Center of Confocal and Electronic Microscopy and CLEM, University "Politecnica delle Marche", Ancona, Italy
[e] International School of Advanced Studies, University of Camerino, Camerino, Italy

ARTICLE INFO

Keywords:
TPC2 channel
Clomipramine
Chlorpromazine
Autophagy
Lysosomal Ca^{2+} homeostasis
ALS/PDC
Drug repurposing

ABSTRACT

Several neurodegenerative diseases including amyotrophic lateral sclerosis (ALS) are characterized by toxic aggregates accumulation due to autophagy blockade, prompting researchers to identify new autophagy-activating drugs. Here we tested, in an *in vitro* ALS/PDC model, the neuroprotective effects of the antipsychotic Chlorpromazine (CPZ) and the antidepressant Clomipramine (CMI), chosen by drug repurposing approach for their ability to stimulate TPC2 lysosomal channel. Patch-clamp electrophysiology on enlarged lysosomes in NSC-34 motor neurons showed that CPZ and CMI induced large inwardly-rectifying currents, that were inhibited by TPC2 synthetic blocker *trans*-Ned-19. The same currents were evoked by TPC2 endogenous agonist NAADP and its mimetic agent TPC2-A1-N, and inhibited by *trans*-Ned-19 and siRNAs against TPC2 (siTPC2). CPZ and CMI elicited a significant $[Ca^{2+}]_i$ increase that rapidly induced nuclear translocation of TFEB (transcription factor EB), the master regulator of autophagy. Accordingly, TPC2 stimulation by both the drugs boosted autophagy, as revealed by the activation of autophagy initiators ULK and AMPK α and modification of LC3-II/p62 (SQSTM1) ratio. Furthermore, by normalizing autophagy markers, CPZ and CMI counteracted the detrimental effects induced by L-BMAA, a neurotoxin mimicking ALS/PDC. Notably, siTPC2 partially reverted CMI- and CPZ-induced neuroprotection as well as that produced by NAADP. At mitochondrial level, these drugs prevented ATP reduction and ROS overproduction in motor neurons exposed to L-BMAA for 24 h. For a longer L-BMAA exposure, CPZ and CMI counteracted LDH, cytochrome *C* and SMAC/DIABLO release, thus preventing cell demise. These findings suggest that TPC2 activation by drug repurposing could provide novel therapeutic options for ALS *via* autophagy regulation.

1. Introduction

The non-protein amino acid beta-methylamino-L-alanine (L-BMAA) is a neurotoxin produced by cyanobacteria, firstly involved in the pathogenesis of Amyotrophic Lateral Sclerosis/Parkinson-Dementia Complex (ALS/PDC), the Guamanian form of the neurodegenerative disease [1]. Moreover, L-BMAA has been also found in the brain of Alzheimer's disease (AD) patients and ALS patients from North America [2], thus suggesting a critical role in other diseases' pathogenesis. Despite the efforts of a plethora of researchers working everywhere in

Abbreviations: CMI, Clomipramine; CPZ, Chlorpromazine; $[Ca^{2+}]_i$, intracellular calcium concentration; L-BMAA, beta-methylamino-L-alanine; ALS/PDC, Amyotrophic Lateral Sclerosis/Parkinson-Dementia Complex; TPC2, Two-Pore Channel 2; NAADP, Nicotinic acid adenine dinucleotide phosphate; TRPML1, TRP mucolipin 1; siRNAs, small interfering RNAs.

* Corresponding author.
E-mail address: a.secondo@staff.univpm.it (A. Secondo).

https://doi.org/10.1016/j.bcp.2025.117219
Received 30 April 2025; Received in revised form 28 July 2025; Accepted 8 August 2025
Available online 10 August 2025

Table 1
List of primary antibodies used in this study.

Antibody	Supplier	Catalog number	Species	Type	Application	Dilution	Tested in:
anti-β-actin-peroxidase	Sigma-Aldrich (Milan, Italy)	A3854 (RRID:AB_262011)	Mouse	Monoclonal	WB	1:10000	Tedeschi *et al.*, FASEB J, 2021; Tedeschi *et al.*, Neurobiol Dis, 2023
anti-AMPK α	Cell Signaling Technology Inc. (Danvers, MA, USA)	2532 (RRID:AB_330331)	Rabbit	Polyclonal	WB	1:1000	Tedeschi *et al.*, Sci Rep, 2019; Sapienza *et al.*, Int J Mol Sci, 2022
anti-phospho-AMPK α (Thr172)	Cell Signaling Technology Inc. (Danvers, MA, USA)	2531 (RRID:AB_330330)	Rabbit	Polyclonal	WB	1:1000	Tedeschi *et al.*, Sci Rep, 2019; Sapienza *et al.*, Int J Mol Sci, 2022; Tedeschi *et al.*, Pharmacol Res, 2024
anti-cytochrome *C*	Cell Signaling Technology Inc. (Danvers, MA, USA)	4272 (RRID:AB_2090454)	Rabbit	Polyclonal	WB	1:1000	Sapienza *et al.*, Int J Mol Sci, 2022; Magliocca *et al.*, Antioxidants, 2024
anti-ERK2	Santa Cruz Biotechnology Inc. (Dallas, TX, USA)	sc-271458 (RRID: AB_10650127)	Mouse	Monoclonal	WB	1:1000	Martin *et al.*, Front Endocrinol, 2016; Tedeschi *et al.*, Pharmacol Res, 2024
anti-histone H3	Thermo Fisher Scientific (Waltham, MA, USA)	PA5-16183 (RRID:AB_10985434)	Rabbit	Polyclonal	WB	1:2000	White C.W. *et al.*, Proc Natl Acad Sci U S A, 2020; Tedeschi V. *et al.*, Pharmacol Res, 2024
anti-LAMP1	Merck Millipore (Darmstadt, Germany)	AB2971 (RRID:AB_11212777)	Rabbit	Polyclonal	WB	1:1000	Tedeschi *et al.*, Sci Rep, 2019; Tedeschi *et al.*, Neurobiol Dis, 2023; Tedeschi *et al.*, Pharmacol Res, 2024
anti-LC3B	GeneTex Inc. (Irvine, CA, USA)	GTX127375 (RRID:AB_11176277)	Rabbit	Polyclonal	WB	1:1000	Tedeschi *et al.*, Sci Rep, 2019; Sapienza *et al.*, Int J Mol Sci, 2022; Tedeschi *et al.*, Neurobiol Dis, 2023; Tedeschi *et al.*, Pharmacol Res, 2024
anti-p62/SQSTM1	Novus Biologicals (Littleton, CO, USA)	NBP1-48320 (RRID:AB_10011069)	Rabbit	Polyclonal	WB	1:1000	Tedeschi *et al.*, Sci Rep, 2019; Sapienza *et al.*, Int J Mol Sci, 2022; Tedeschi *et al.*, Neurobiol Dis, 2023: Tedeschi *et al.*, Pharmacol Res, 2024
anti-SMAC/DIABLO	abcam (Cambridge, UK)	ab111893 (RRID: AB_10862924)	Mouse	Monoclonal	WB	1:1000	Magliocca *et al.*, Antioxidants, 2024
anti-TFEB	GeneTex Inc. (Irvine, CA, USA)	GTX33541 (RRID:AB_2887718)	Rabbit	Polyclonal	WB ICC	1:1000 1:300	Bisicchia E. *et al.*, Cell Death Dis, 2022; Tedeschi V. *et al.*, Pharmacol Res, 2024
anti-TPC2	Alomone Labs (Jerusalem, Israel)	ACC-072 (RRID:AB_10918019)	Rabbit	Polyclonal	WB ICC	1:1000 1:1000	Tedeschi *et al.*, Neurobiol Dis, 2023
anti-phospho-ULK (Ser317)	MyBioSource Inc. (San Diego, CA, USA)	MBS9600629 (RRID: not available)	Rabbit	Polyclonal	WB	1:1000	Tedeschi *et al.*, Pharmacol Res, 2024

Application. WB: Western blotting; ICC: immunocytochemistry.

the search for a cure, there is no useful pharmacological therapy for most of the neurodegenerative diseases −including ALS- which remain unmet medical needs.

"Drug repurposing", also defined as "drug repositioning", is aimed at identifying new pharmacological uses for existing drugs or prodrugs previously approved for other indications [3,4]. Since the pharmacokinetics, pharmacodynamics, and toxicity profile of repurposed candidates are already known, the main advantage of drug repurposing is to bypass some development steps of the clinical trials proceeding directly to the phase II. Two main modalities for "drug repurposing" exist: the On-target- and the Off-target-strategies. In the first case, an already known molecular entity with a specific mechanism is applied to a different disease [5], while in the Off-target repurposing, an old drug is considered for a new mechanism, previously recognized as a side effect [6].

In the context of the neurological drugs, some antipsychotics, alone or in combination with other molecular entities, have shown to produce or improve therapeutic effects on cortical myelination in multiple sclerosis (MS) models [7] as well as spatial working memory and locomotor activity potentiation [8–11]. This seems to occur *via* autophagy modulation [7], a process highly affected in the neurodegenerative diseases and now considered as a causative mechanism for most of them [12]. Autophagy process is differently related to each neurodegenerative disease: it can be hypofunctional or blocked, thus reducing the clearing capacity of neurons and producing cell death, as actually occurs in Parkinson's disease (PD) [13], Alzheimer's disease (AD) [14], Huntington's disease (HD) [15] and ALS [12,16,17] or hyperfunctional, as occurs in Stroke [18] and MS. In the latter case, an excessive autophagy in astrocytes may lead to apoptosis and aggravates inflammation [19]. Moreover, significant inhibition of autophagy in oligodendrocyte precursor cells could be detrimental to myelin regeneration [20,21]. This is indicative of an opposite role of autophagy depending on the disease phase and cell type involved.

With the aim to add new knowledge on the role of autophagy in each neurodegenerative disease, it has been reported that the control hub of the process is the lysosome, a tiny organelle storing Ca^{2+} ions with a complex machinery. In particular, two lysosomal cationic channels named TRP mucolipin 1 (TRPML1) [22] and Two-Pore Channel 2 (TPC2) [23] have been found to preside autophagy in neurons by releasing Ca^{2+}, activating calcineurin and triggering nuclear translocation of the transcription factor EB (TFEB), that is considered as the master regulator of this cleansing process [22]. It is quite well accepted that TPC2 is rather Ca^{2+} and Na^{+} selective [24–26]. It can be activated by two different agonists, namely $PI(3,5)P_2$ and NAADP that, respectively, lead to Na^{+}- or Ca^{2+}- current activation [27]. Moreover, only TPC2-mediated Ca^{2+} movement may trigger protective autophagy in Lysosomal Storage Diseases (LSDs) [28,29]. Of note, the tricyclic antidepressant (TCA) clomipramine (CMI) and the antipsychotic chlorpromazine (CPZ) have been characterized for their ability to stimulate TPC2 in non-neuronal cells [25].

In consideration of this pharmacological evidence, the effect of clomipramine and chlorpromazine has been studied in a model of ALS/PDC, in which autophagy blockade is considered as one of the main causative mechanisms [16]. This peculiar form of the disease may share with ALS and PD, as well as several LSDs, the accumulation of toxic aggregates due to autophagy dysfunction, thus rendering each autophagy-activating drug a good candidate for therapy.

In the present manuscript we tested, *in vitro,* the putative neuroprotective effects of clomipramine and chlorpromazine in a model of ALS/PDC reproduced by exposing motor neurons to the neurotoxin L-BMAA. Here, the involvement of TPC2-mediated autophagy has been investigated with the aim to (*i*) expand the therapeutic value of the drugs

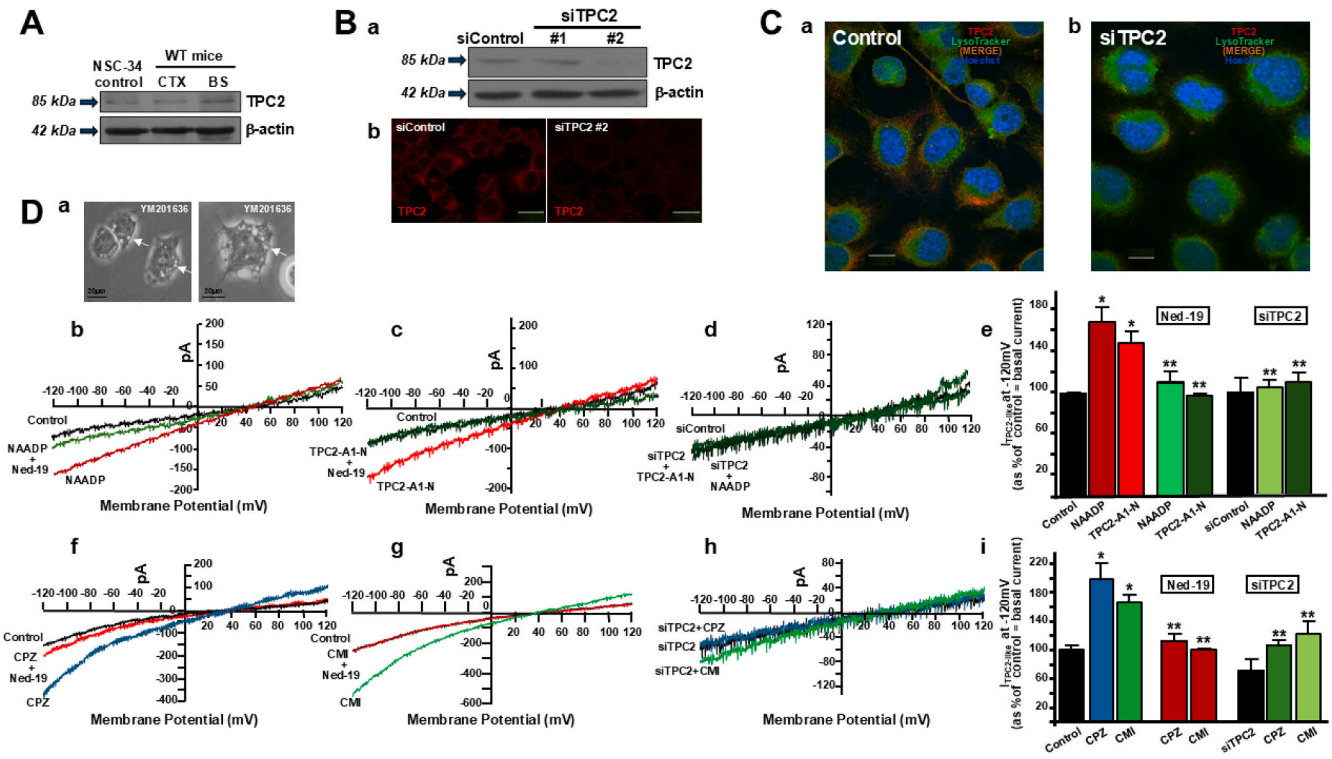

Fig. 1. Clomipramine and chlorpromazine stimulated TPC2 activity in NSC-34 motor neuronal cells under physiological conditions. (A) Representative Western blotting of TPC2 expression in NSC-34 motor neurons under control conditions and in cortex (CTX) and brainstem (BS) isolated from wild-type mice. (B) Representative Western blotting of TPC2 expression in NSC-34 motor neurons treated with siControl or two different siRNAs (a); TPC2 immunostaining in NSC-34 cells treated with siControl or siRNA #2; Scale bar: 20 μm (b). (C) Co-localization between TPC2 and Lysotracker Green in NSC-34 motor neurons under control conditions (a) and after siTPC2 #2 exposure for 48 h; Scale bar: 10 μm. (b). (D) Representative brightfield images of NSC-34 motor neurons treated with YM201636 (1 μM/2h) (a); representative whole-lysosome currents and quantification in basal conditions and after NAADP-AM (1 μM) administration, in the absence or presence of Ned-19 (30 μM), (n = 5 endolysosomes for each group of NSC-34 cells) (b,e); representative whole-lysosome currents and quantification in basal conditions and after TPC2-A1-N administration (8 μM) in the absence or presence of Ned-19 (30 μM), (n = 5 endolysosomes for each group of NSC-34 cells) (c,e); representative whole-lysosome currents and quantification in siControl- or siTPC2 #2-treated cells (48 h for both) (n = 5 endolysosomes for each group of NSC-34 cells) (d,e); representative whole-lysosome currents and quantification in basal conditions and after CPZ (20 μM) administration, in the absence or presence of Ned-19 (30 μM), (n = 6 endolysosomes for each group of NSC-34 cells) (f,i); representative whole-lysosome currents and quantification in basal conditions and after CMI (4 μM) administration, in the absence or presence of Ned-19 (30 μM), (n = 6 endolysosomes for each group of NSC-34 cells) (g,i); representative whole-lysosome currents and quantification in siTPC2 #2-treated cells (48 h for both) exposed to each drug (n = 5 endolysosomes for each group of NSC-34 cells) (h,i). Each bar represents the mean ± S.E.M. of data obtained from three different experimental sessions. *p < 0.01 vs basal currents; **p < 0.01 vs each internal control (NAADP or TPC2-A1-N in e or CPZ or CMI alone in i). (For interpretation of the references to colour in this figure legend, the reader is referred to the web version of this article.)

and (*ii*) identify a new pharmacological target in the neurodegeneration induced by L-BMAA.

2. Materials and methods

2.1. Reagents

Media and supplements for cell cultures were from Gibco (ThermoFisher Scientific Inc., Waltham, MA, USA). Clomipramine, chlorpromazine, L-BMAA, rotenone, MTT, 2′,7′-dichlorodihydrofluorescein diacetate (DCF-DA), bafilomycin A1, ionomycin and the ATP bioluminescent assay kit were purchased from Sigma-Aldrich (Merck Millipore, Milan, Italy). YM201636 was from Santa Cruz Biotechnology, Inc. (Dallas, TX, USA). NAADP-AM was from AAT Bioquest (Sunnyvale, CA, USA). *trans*-Ned-19 (referred to as Ned-19 in the figures) was from Tocris Bioscience (Bristol, UK). Fluo-4AM and LysoTracker™ Green DND-26 were from Molecular Probes (Invitrogen, ThermoFisher Scientific Inc., Waltham, MA, USA). ECL reagents and nitrocellulose membranes were from Cytiva Amersham (Amersham, UK). The Cytotoxicity LDH assay Kit-WST was purchased from Dojindo (Kumamoto, Japan). Small interfering RNAs (siRNAs) against TPC2, TRPML1 and siRNA-Control were purchased from Qiagen (Milan, Italy). TPC2-A1-N was from MedChem Express (Monmouth Junction, NJ, USA).

2.2. Cell cultures and treatments

NSC-34 motor neuronal cells [30] were grown in Dulbecco's Modified Eagles Medium containing 4.5 g/L glucose and supplemented with 10 % fetal bovine serum (FBS), 2 mM L-glutamine, 100 IU/mL penicillin and 100 μg/mL streptomycin. Cells, plated in Petri dishes, in multiple well cluster plates or on glass coverslips, were kept in a 5 % CO_2 and 95 % air atmosphere at 37° C, as previously described [16,31]. In order to reproduce an *in vitro* model of Amyotrophic Lateral Sclerosis/Parkinson-Dementia Complex (ALS/PDC), NSC-34 cells were chronically exposed to the cycad neurotoxin β-methylamino-L-alanine (L-BMAA) (300 μM/48 h) in Minimum Essential Medium (MEM) supplemented with 10 % FBS, 2 mM L-glutamine, 100 IU/mL penicillin and 100 μg/mL streptomycin.

Primary cortical neurons were obtained from brains of 14/16-day-old Wistar rat embryos, as previously reported [18].

In order to achieve TPC2 protein knocking-down, motor neuronal cells were transfected with four different FlexiTube small interfering RNAs (siRNAs) against the lysosomal Ca^{2+} channel TPC2 (all at 10 nM):

- (#1) Mm_Tpcn2_1 (SI01454019; target sequence: CAGGCTGTGGTCTTCATTGAA)

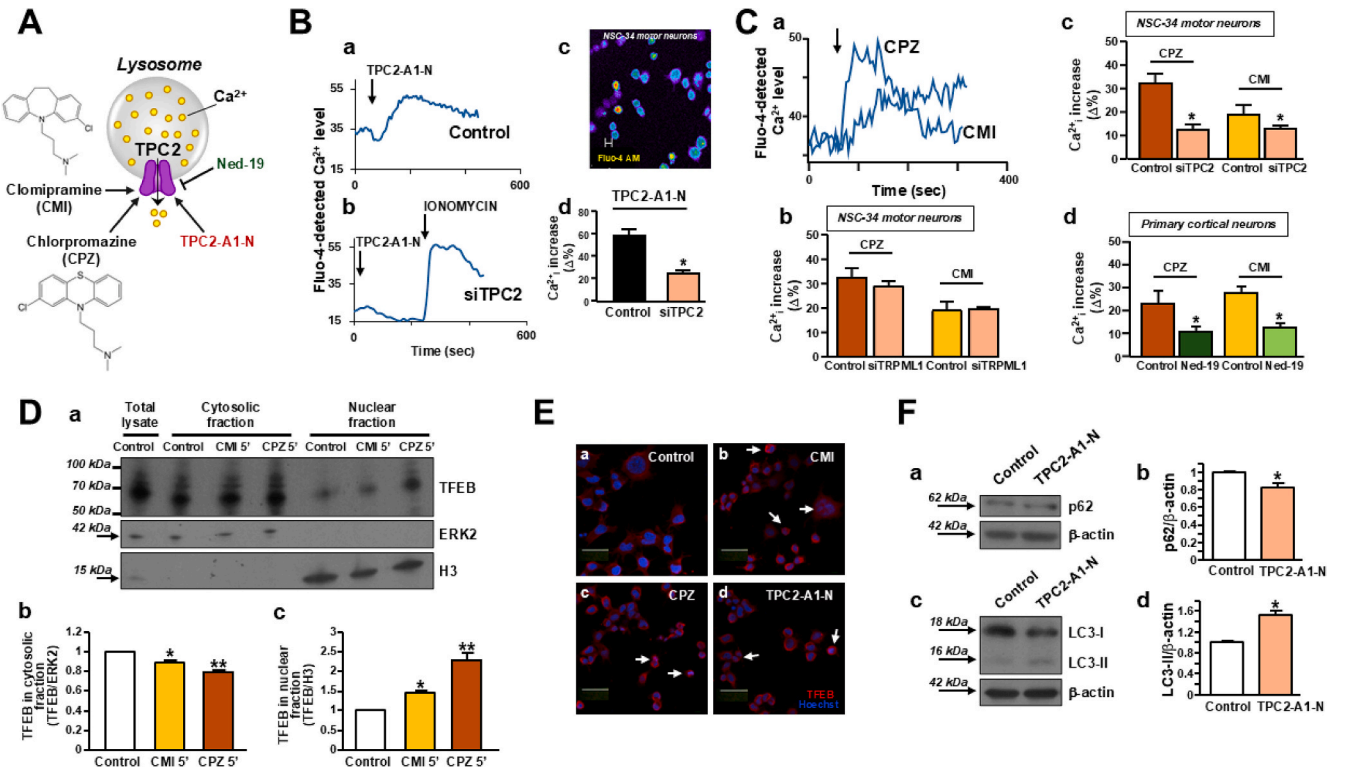

Fig. 2. Clomipramine and chlorpromazine stimulated Ca^{2+} release from lysosomal TPC2 and TFEB nuclear translocation in NSC-34 motor neuronal cells under physiological conditions. (A) Representative cartoon of lysosomal TPC2 activation by clomipramine (CMI), chlorpromazine (CPZ) or TPC2-A1-N and TPC2 inhibition by *trans*-Ned-19. (B) Representative traces (a,b) and quantification (d) of the effect on intracellular Ca^{2+} concentration ($[Ca^{2+}]_i$) of TPC2-A1-N (8 μM) in cells under control conditions or treated with siTPC2 #2. In the latter case, cell viability has been tested by ionomycin at the end of the recording. *$p < 0.01$ vs control; (c) representative image in pseudocolor of NSC-34 motor neuronal cells loaded with Fluo-4AM; Scale bar: 20 μm. (C) Superimposed traces representative of the effect of CMI (4 μM) and CPZ (20 μM) on $[Ca^{2+}]_i$ in motor neurons under physiological conditions (a); quantification of their effects as Δ % of increase over basal Ca^{2+} levels in motor neuronal cells treated with siTRPML1 (b) or siTPC2 #2 (c) or in primary cortical neurons at 7 DIV (d). Each bar represents the drug effect reported as mean ± S.E.M. ($n = 20–25$ cells for each group recorded in three different experimental sessions); *$p < 0.01$ vs each internal control (CPZ or CMI alone). (D) Representative Western blotting of TFEB expression (a) and quantification (b,c) in total lysate of NSC-34 motor neurons or in their cytosolic and nuclear fractions after 5 min exposure to CPZ or CMI. Data are expressed as mean ± S.E.M. of three different experimental sessions. *$p < 0.05$ vs control, **$p < 0.05$ vs control and CMI 5′. (E) TFEB immunosignal in NSC-34 cells under control conditions (a), after 5 min exposure to CMI (4 μM) (b), after 5 min exposure to CPZ (20 μM) (c) or after 5 min exposure to TPC2-A1-N (8 μM) (d). Arrows indicate representative cells showing TFEB nuclear localization. (F) Representative Western blotting (a,c) and quantification (b,d) of p62 and LC3-II expression in motor neurons treated with TPC2-A1-N (8 μM). *$p < 0.05$ vs each internal control.

- (#2) Mm_Tpcn2_2 (SI01454026; target sequence: CAGCCTGGTTCCCGACAACAA)
- (#3) Mm_Tpcn2_3 (SI01454033; target sequence: CTGGCTGATGAGTTCCAGAAA)
- (#4) Mm_Tpcn2_4 (SI01454040; target sequence: AGGAAGCTTGTTTCTGATGAA)

and with the non-targeting control (Qiagen, Milan, Italy). TPC2 protein expression levels were significantly reduced only by using siRNA #2.

Furthermore, TRPML1 knocking-down was achieved as already published [16] by the following FlexiTube siRNA (Qiagen, Milan, Italy):

- Mm_Mcoln1_5 (SI02696855; sense strand: 5′-CAAGAACCUCACACUGAAATT-3′; antisense strand: 5′-UUUCAGUGUGAGGUUCUUGTA-3′) (10 nM).

2.3. Western blotting experiments

Cells or tissues were lysed in an ice-cold lysis buffer containing 100 mM NaCl, 50 mM Tris-HCl (pH 7.4), 0.2 % SDS, 0.5 % NP-40, 1 mM EGTA, 1 mM PMSF, 1 mM Na_3VO_4, 1 mM NaF, and a protease inhibitor mixture (Roche Diagnostics, Monza, IT). After lysis, total proteins (20–30 μg) from each sample were separated by sodium dodecyl sulphate–polyacrylamide gel electrophoresis and then electrotransferred onto 0.2 μm nitrocellulose membranes. The primary antibodies used in this study are listed in Table 1.

For tissue lysates, cortices and brainstems were isolated from wild-type mice (B6SJL, Jackson Laboratories, Bar Harbor, USA). All the procedures, performed in accordance with the European Guidelines for the use of animals in research (2010/63/EU) and the requirements of Italian laws (D.L. 26/2014), were approved by the Animal Care Committee of "Federico II" University of Naples and the Animal welfare office, Department of Public Health and Veterinary, Nutrition and Food Safety, General Management of Animal Care and Veterinary Drugs of the Italian Ministry of Health (589/2020-PR). All efforts were made to minimize animal suffering and to reduce the number of animals.

2.4. Immunocytochemistry on cell cultures

For immunocytochemistry, NSC-34 motor neurons were fixed at room temperature in 4 % paraformaldehyde for 20 min as previously reported [16]. Briefly, following several washes in PBS, cells were blocked in 3 % BSA for 30 min and then incubated with TPC2 or TFEB antibody overnight. For the colocalization experiments, cells exposed to TPC2 were treated also with Lysotracker Green for 20 min and, then, incubated with Hoechst for the last 5 min. Controls of the method included the replacement of each primary antibody with normal serum.

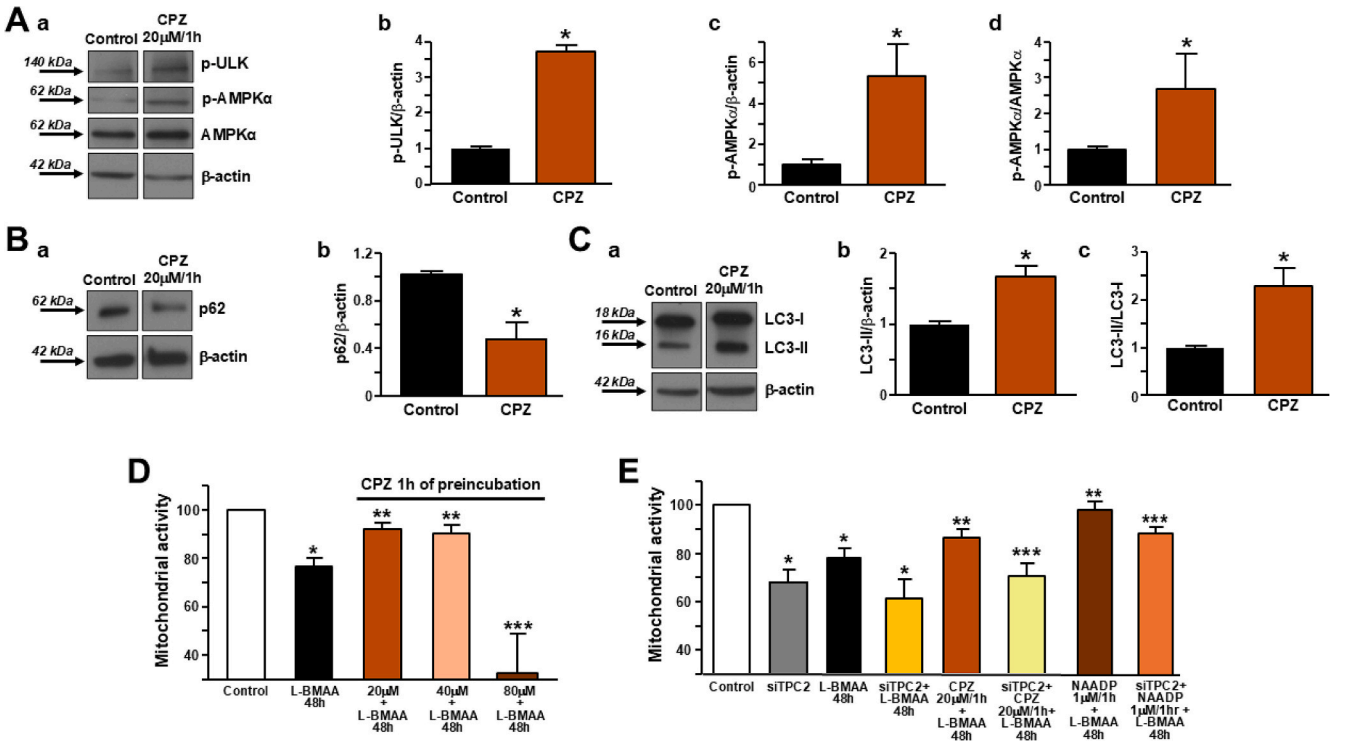

Fig. 3. Chlorpromazine promoted the activation of the autophagic flux in NSC-34 motor neuronal cells under physiological conditions and protected motor neurons against L-BMAA-induced mitochondrial dysfunction. (A) Representative Western blotting (a) and quantification of phospho-ULK (p-ULK) (b) and phospho-AMPK α (p-AMPK α) (c-d) expression in motor neurons treated with CPZ (20 μM/1h). Data are expressed as mean ± S.E.M. of three different experimental sessions. *$p < 0.05$ vs control. (B) Representative Western blotting (a) and quantification of p62 expression (b) in motor neurons treated with CPZ (20 μM/1h). Data are expressed as mean ± S.E.M. of three different experimental sessions. *$p < 0.05$ vs control. (C) Representative Western blotting (a) and quantification of LC3-II expression (b-c) in motor neurons treated with CPZ (20 μM/1h). Data are expressed as mean ± S.E.M. of three different experimental sessions. *$p < 0.05$ vs control. (D) Bar graph depicting the effect of CPZ (20 μM, 40 μM and 80 μM, preincubated for 1 h) on mitochondrial activity in NSC-34 motor neurons chronically exposed to the neurotoxin L-BMAA (300 μM/48 h). Data are expressed as mean ± S.E.M. of three different experimental sessions. *$p < 0.05$ vs control; ** $p < 0.05$ vs L-BMAA 48 h; ***$p < 0.05$ vs all. (E) Bar graph depicting the effect of CPZ (20 μM preincubated for 1 h) and NAADP (1 μM preincubated for 1 h) on mitochondrial activity in NSC-34 motor neurons chronically exposed to the neurotoxin L-BMAA (300 μM/48 h) and previously silenced for TPC2 expression by a specific siRNA against the channel (siTPC2). Data are expressed as mean ± S.E.M. of three different experimental sessions. *$p < 0.05$ vs control; ** $p < 0.05$ vs L-BMAA 48 h; ***$p < 0.05$ vs L-BMAA + CPZ or vs L-BMAA + NAADP.

Cover glasses were mounted with a SlowFade Antifade Kit (Molecular Probes, Life Technologies, Milan, Italy). Images were acquired with an inverted microscope Eclipse Ti2-E supplied with an AX confocal system (Nikon, Japan) at 60x magnification.

2.5. Electrophysiology on lysosomes

The whole-endolysosome configuration was achieved by a modified patch-clamp method [32–35], as previously described [17]. Briefly, whole-endolysosome recordings in NSC-34 cells were performed on vacuoles enlarged by treating cells with 1 μM YM201636 for at least 2 h. The pipette (luminal) solution contained (in mM): 145Na-gluconate, 5 KCl, 2 $CaCl_2$, 1 $MgCl_2$, 10 HEPES, 10 MES and 10 glucose (pH 4.6 with NaOH), and bath (cytoplasmic) solution contained (in mM): 140 K-Gluconate, 4 NaCl, 1 EGTA, 2 $MgCl_2$, 0.39 $CaCl_2$, 0.1 GTP and 10 HEPES (pH 7.2 with KOH and $[Ca^{2+}]_i$ of 100 nM). Cells were held at 0 mV and the currents were elicited by repeated voltage ramps (from − 140 to + 140 mV; 400 ms) with a 4-s interval between ramps. Bath application of NAADP-AM (1 μM), TPC2-A1-N (8 μM), clomipramine (4 μM) or chlorpromazine (20 μM) induced the activation of TPC2-mediated currents (I_{TPC2}). I_{TPC2} were recorded using the commercially available amplifier Axopatch 200B and Digidata 1322 A interface (Molecular Devices). Data were acquired and analyzed using the pClamp software (version 10, Molecular Devices). Whole-endolysosome currents were digitized at 10 kHz and filtered at 2 kHz. All the experiments were conducted at room temperature (21-23° C) in the absence of ATP. The recordings were analyzed in pCLAMP10 (Molecular Devices, CA, USA).

2.6. Ca^{2+} imaging on single-cell

$[Ca^{2+}]_i$ was detected by single-cell video-imaging experiments in NSC-34 motor neurons or in primary cortical neurons isolated from Wistar rat embryos as previously described [18]. Cells, plated on glass coverslips, were loaded with the non-ratiometric fluorescent Ca^{2+} indicator Fluo-4AM (10 μM) [36] for 45 min at 37° C. At the end of the loading period, the coverslips were placed into a perfusion chamber (Medical System, Greenvale, NY, USA) mounted onto a Zeiss Axiovert 200 fluorescence microscope (Carl Zeiss) equipped with a 40x oil objective lens. Cells were illuminated at 488 nm wavelength and the emitted light was passed through a 512 nm barrier filter. Fluo-4 fluorescence intensity was measured every 3 s. The effect of clomipramine and chlorpromazine on $[Ca^{2+}]_i$ was evaluated as Δ% of increase over basal Ca^{2+} levels. Experiments were repeated 3 times on at least 20 cells.

2.7. Cell viability

Cell viability was assessed as mitochondrial activity by using the 3 [4,5-dimethylthiazol-2-yl]-2,5-diphenyl-tetrazolium bromide (MTT) assay, as previously reported [37]. Data are expressed as a percentage of cell viability compared to control cultures.

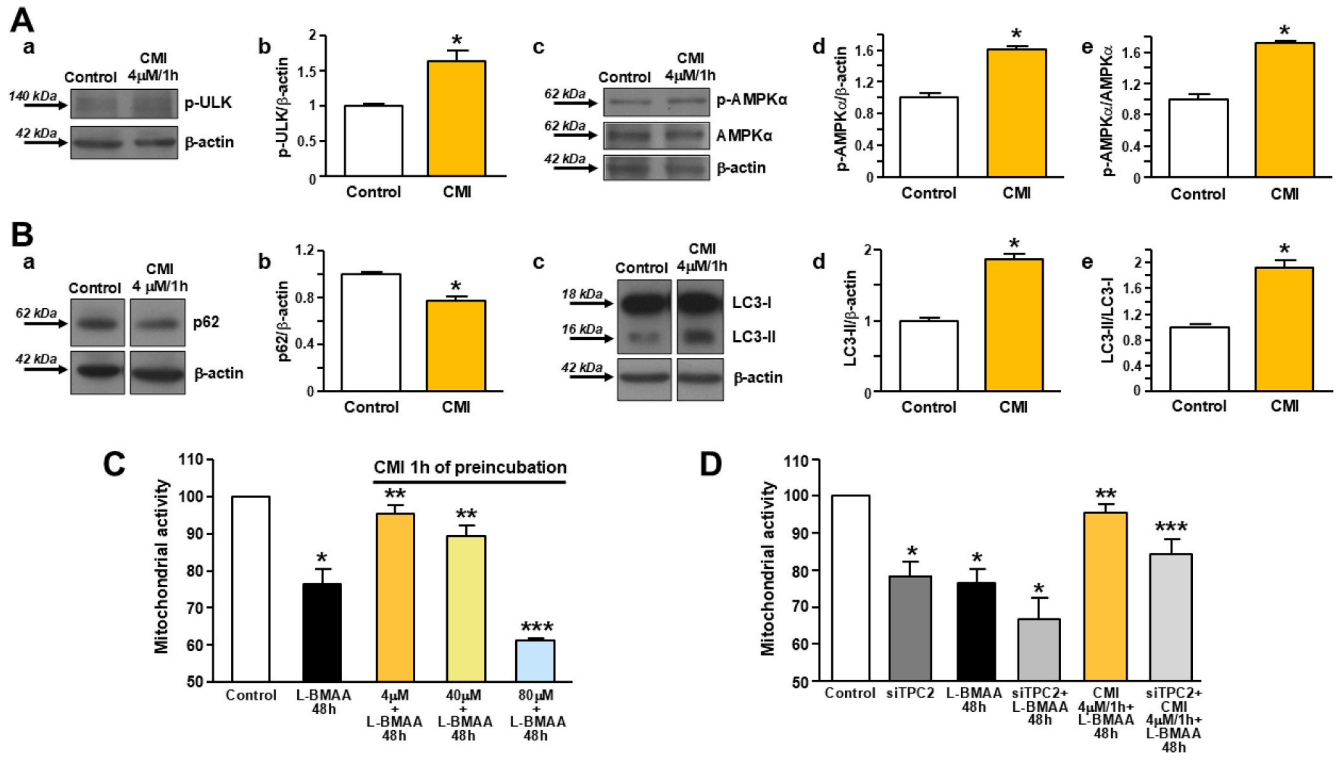

Fig. 4. Clomipramine promoted the activation of the autophagic flux in NSC-34 motor neuronal cells under physiological conditions and protected motor neurons against L-BMAA-induced mitochondrial dysfunction. (A) Representative Western blotting and quantification of phospho-ULK (p-ULK) (a-b) and phospho-AMPK α (p-AMPK α) expression (c-e) in motor neurons treated with CMI (4 μM/1h). Data are expressed as mean ± S.E.M. of three different experimental sessions. *p < 0.05 vs control. (B) Representative Western blotting and quantification of p62 (a-b) and LC3-II expression (c-e) in motor neurons treated with CMI (4 μM/1h). Data are expressed as mean ± S.E.M. of three different experimental sessions. *p < 0.05 vs control. (C) Bar graph depicting the effect of CMI (4 μM, 40 μM and 80 μM, preincubated for 1 h) on mitochondrial activity in NSC-34 motor neurons chronically exposed to the neurotoxin L-BMAA (300 μM/48 h). Data are expressed as mean ± S.E.M. of three different experimental sessions. *p < 0.05 vs control; ** p < 0.05 vs L-BMAA 48 h; ***p < 0.05 vs all. (D) Bar graph depicting the effect of CMI (4 μM, preincubated for 1 h) on mitochondrial activity in NSC-34 motor neurons chronically exposed to the neurotoxin L-BMAA (300 μM/48 h) and previously silenced for TPC2 expression by a specific siRNA against the channel (siTPC2). Data are expressed as mean ± S.E.M. of three different experimental sessions. *p < 0.05 vs control; ** p < 0.05 vs L-BMAA 48 h; ***p < 0.05 vs L-BMAA + CMI.

2.8. Quantification of ATP content

ATP content was measured by using an ATP bioluminescent assay kit (Sigma-Aldrich, Milan, Italy), as previously described [37]. Briefly, ATP was extracted by boiling the samples in a solution containing 100 mM TRIS, 4 mM EDTA, pH 7.75. Samples were centrifugated at 10,000 × g for 60 sec and then diluted in a dilution buffer (1:50). To obtain the bioluminescence measurements with a standard luminometer, 50 μL of supernatant were mixed with 50 μL of luciferin-luciferase solution. The standard ATP curve was obtained by serial dilutions of a 2 μM ATP solution.

2.9. Intracellular ROS measurement by cytofluorimetry

Intracellular reactive oxygen species (ROS) production was measured in NSC-34 cells using the fluorescent probe 2′,7′-dichloro-fluorescein-diacetate (DCF-DA), as previously described [38]. After reaching the exponential phase of growth, cells were collected, washed twice, and then incubated in PBS containing DCF-DA (5 μM) at 37° C for 30 min. Flow cytometry evaluation was performed by using the ATTUNE NxT acoustic focusing cytometer (Life Technologies, Carlsbad, CA, USA). Data analysis was performed by using FlowJo Software (FlowJo, LLC, Ashland, OR, USA) [39]. The intracellular ROS levels were expressed as mean fluorescence intensity.

2.10. Lactate dehydrogenase (LDH) release assay

LDH release was measured using the Cytotoxicity LDH assay Kit-WST (Dojindo, Kumamoto, Japan) according to the manufacturer's instructions. Cytotoxicity was calculated as a percentage of the ratio of LDH released in the extracellular medium compared to intracellular LDH released after cell lysis, as previously described [18].

2.11. Cytosolic lysates and nuclear-cytoplasmic fractionation

Cells were lysed in an ice-cold lysis buffer (10 mM HEPES pH 7.9-KOH, 10 mM KCl, 1,5 mM $MgCl_2$, 100 mM EGTA, 500 mM DTT, 1 mM Na_3VO_4, 200 mM PMSF, 10 % glycerol) supplemented with a protease inhibitor mixture (Roche Diagnostics, Monza, IT). The lysates were passed at least 10 times through a 30G needle using a 1 mL syringe and then centrifugated for 5 min at 3000 rpm, 4° C. The resulting supernatant, representing the cytosolic fraction, was analyzed for cytochrome *C* and SMAC/DIABLO protein expression by Western blotting experiments.

Nuclear-cytoplasmic fractionations were prepared using an ice-cold lysis buffer (100 mM NaCl, 50 mM Tris-HCl pH 7.4, 0,2 % SDS, 1 mM EGTA, 1 mM NaF, 1 mM phenylmethylsulfonyl fluoride, 0,5 % NONIDET P-40, 1 mM Na_3VO_4) containing a protease inhibitor mixture. Then, the lysate was centrifuged for 5 min at 500 g, 4° C. The resulting pellets contained nuclear fractions that were lysed in RIPA buffer and sonicated.

2.12. Statistical analyses

Data are expressed as mean ± SEM. Statistical analysis was performed with unpaired *t* test or one-way analysis of variance followed by

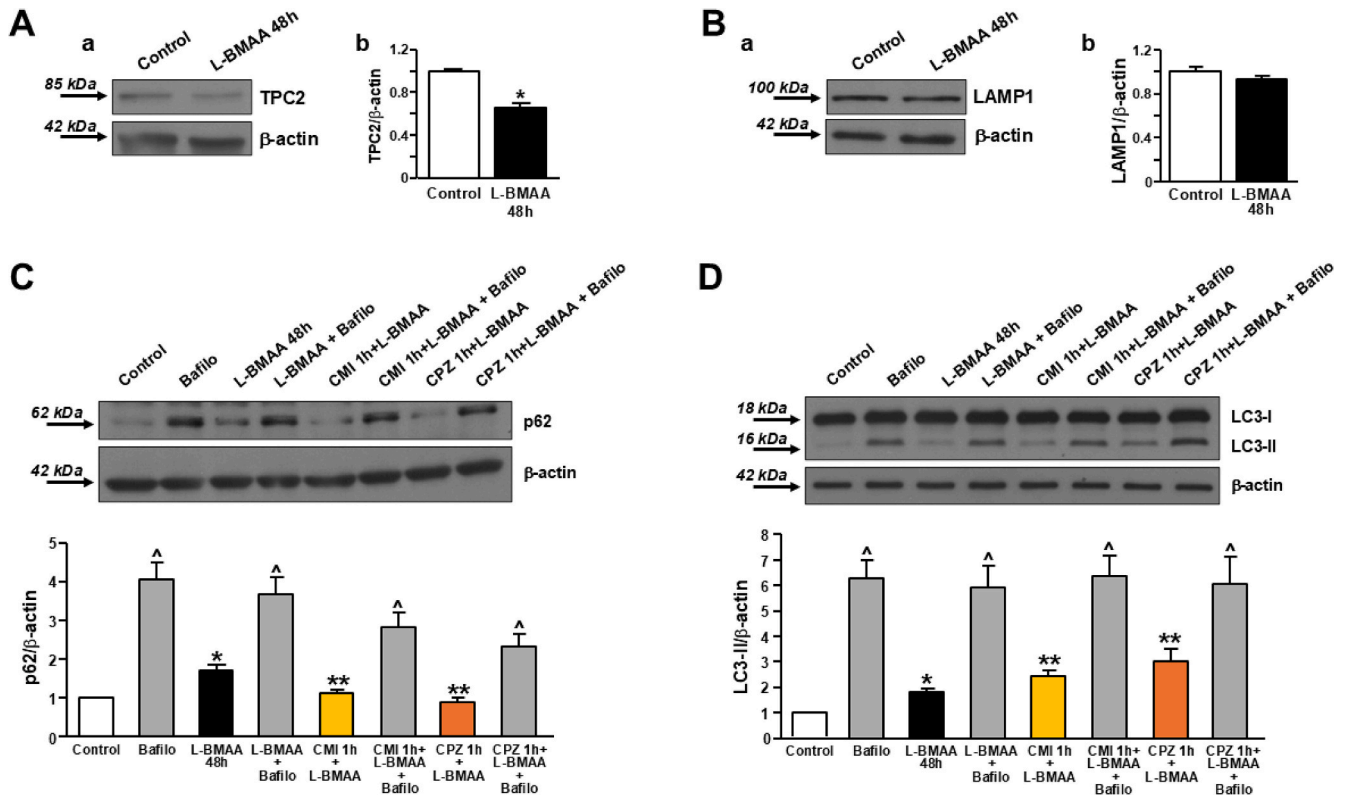

Fig. 5. Clomipramine and chlorpromazine boosted autophagy flux in NSC-34 motor neurons chronically exposed to the neurotoxin L-BMAA. (A) Representative Western blotting (a) and quantification (b) of TPC2 expression under control conditions and after L-BMAA exposure (48 h). Data are expressed as mean ± S.E.M. of three different experimental sessions. *p < 0.05 vs control. (B) Representative Western blotting (a) and quantification (b) of LAMP1 expression under control conditions and after L-BMAA exposure (48 h). Data are expressed as mean ± S.E.M. of three different experimental sessions. (C) Representative Western blotting (top) and quantification (bottom) of p62 expression in L-BMAA-exposed motor neurons previously incubated with CMI (4 μM/1h) or CPZ (20 μM/1h) in the absence or presence of bafilomycin. Data are expressed as mean ± S.E.M. of three different experimental sessions.^p < 0.01 vs each internal control; *p < 0.05 vs control (NSC-34 cells under physiological conditions); ** p < 0.05 vs L-BMAA 48 h. (D) Representative Western blotting (top) and quantification (bottom) of LC3-II expression in L-BMAA-exposed motor neurons previously incubated with CMI (4 μM/1h) or CPZ (20 μM/1h) in the absence or presence of bafilomycin. Data are expressed as mean ± S.E.M. of three different experimental sessions.^p < 0.01 vs each internal control; * p < 0.05 vs control (NSC-34 cells under physiological conditions); ** p < 0.05 vs L-BMAA 48 h.

Newman-Keuls test. Differences were considered statistically significant when the *p* value was < 0.05.

3. Results

3.1. Clomipramine (CMI) and chlorpromazine (CPZ) stimulated lysosomal TPC2 and increased $[Ca^{2+}]_i$ in NSC-34 motor neuronal cells and primary cortical neurons

Two-Pore Channel 2 (TPC2) represents one of the most relevant cationic channels at lysosomal level. TPC2 protein was highly expressed in NSC-34 motor neuronal cells as well as in mouse cortex and brainstem (Fig. 1A), two brain regions containing motor neurons. TPC2 protein expression as well as its immunosignal were significantly reduced by FlexiTube siRNA #2 (in arbitrary units: 0.45 ± 0.007 for siTPC2 vs 1 for siControl; *p < 0.05; Fig. 1B, a,b). Under control conditions, TPC2 immunosignal displayed a punctuate signal (Fig. 1B, b) that co-localized with a large part of the lysosomes, as revealed by the overlay between Lysotracker Green and TPC2 immunosignal in red (Fig. 1C, a). Of note, this co-localization largely disappeared in motor neuronal cells treated with siTPC2 #2 (Fig. 1C, b).

With the aim to study the modulatory effect of the antipsychotic drug Chlorpromazine (CPZ) and the TCA Clomipramine (CMI) on TPC2 activity in NSC-34 motor neuronal cells, electrophysiological characterization of TPC2-mediated currents was performed by whole-endolysosome configuration method and single-cell Ca^{2+} imaging. Patch-clamp experiments on enlarged lysosomes (Fig. 1D, a) −achieved by a modified patch-clamp method- showed that the cell permeant form of the endogenous TPC2 agonist, NAADP-AM, induced large inwardly-rectifying currents that were inhibited by the synthetic blocker of the channel *trans*-Ned-19 (Ned-19; Fig. 1D, b,e) and siTPC2 #2 (Fig. 1D, d, e). As a positive control, the synthetic NAADP mimetic agonist TPC2-A1-N [27] produced a superimposable stimulating effect that was reduced by *trans*-Ned-19 (Fig. 1D, c,e) and siTPC2 #2 (Fig. 1D, d,e). Moreover, the same protocol was applied for the study of CPZ and CMI on TPC2-mediated currents in NSC-34 motor neuronal cells. In accordance to the modulatory role of these drugs on TPC2 activity in other models [25], CPZ and CMI mimicked the same electrophysiological effect of NAADP-AM and TPC2-A1-N thus eliciting large inwardly-rectifying currents (Fig. 1 D f,g,i) that were reduced by *trans*-Ned-19 (Fig. 1D, f, g,i) and siTPC2 #2 (Fig. 1D, h,i). Considering the Ca^{2+}-selective nature of NAADP at TPC2 level, its mimetic agent TPC2-A1-N induced a rapid increase of intracellular Ca^{2+} level that was significantly prevented by siTPC2 (Fig. 2B, a,b,d). Furthermore, CPZ and CMI mimicked the same effect inducing a rapid increase of intracellular Ca^{2+} level that was significantly prevented by siTPC2 but not by siTRPML1 (Fig. 2C, a-c), as revealed by Fluo-4 measurements in NSC-34 motor neurons. Of note, CPZ and CMI induced a rapid increase of intracellular Ca^{2+} levels also in primary cortical neurons that was prevented by *trans*-Ned-19 (Fig. 2C, d). Consequently, as downstream effect of lysosomal Ca^{2+} release, the two drugs triggered a rapid nuclear translocation of TFEB, as revealed in nuclear preparations of motor neurons exposed to each drug for 5 min

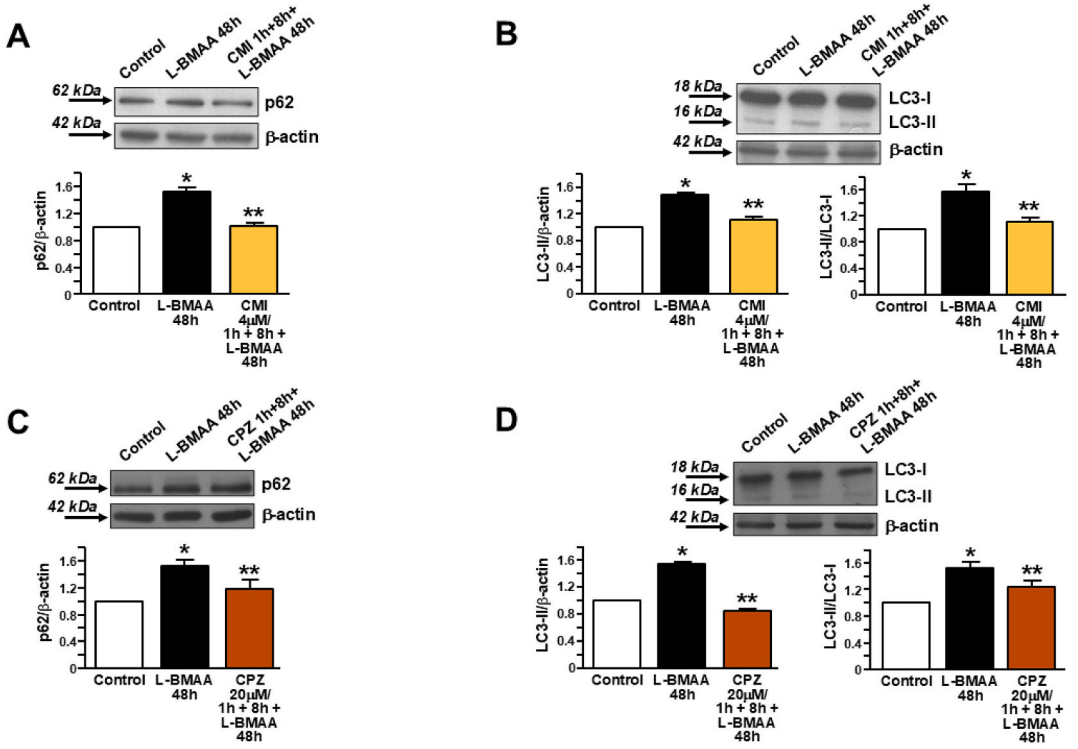

Fig. 6. Clomipramine and chlorpromazine washout restored the autophagic flux in NSC-34 motor neurons chronically exposed to the neurotoxin L-BMAA. (A) Representative Western blotting (top) and quantification (bottom) of p62 expression in L-BMAA-treated motor neurons previously incubated with CMI (4 μM/1h). After 8 h, cells were exposed to L-BMAA. Data are expressed as mean ± S.E.M. of three different experimental sessions. *p < 0.05 vs control; ** p < 0.05 vs L-BMAA 48 h. (B) Representative Western blotting (top) and quantification (bottom) of LC3-II expression in L-BMAA-treated motor neurons previously incubated with CMI (4 μM/1h). After 8 h, cells were exposed to L-BMAA. Data are expressed as mean ± S.E.M. of three different experimental sessions. *p < 0.05 vs control; ** p < 0.05 vs L-BMAA 48 h. (C) Representative Western blotting (top) and quantification (bottom) of p62 expression in motor neurons treated with L-BMAA (300 μM/48 h) and previously incubated with CPZ (20 μM/1h). After 8 h, cells were exposed to L-BMAA. Data are expressed as mean ± S.E.M. of three different experimental sessions. *p < 0.05 vs control; ** p < 0.05 vs L-BMAA 48 h. (D) Representative Western blotting (top) and quantification (bottom) of LC3-II expression in motor neurons treated with L-BMAA (300 μM/48 h) and previously incubated with CPZ (20 μM/1h). After 8 h, cells were exposed to L-BMAA. Data are expressed as mean ± S.E.M. of three different experimental sessions. *p < 0.05 vs control; ** p < 0.05 vs L-BMAA 48 h.

(Fig. 2D, a-c). Furthermore, CMI, CPZ and TPC2-A1-N determined a significant change in TFEB immunosignal that appeared with a typical nuclear localization compared with untreated control (Fig. 2E, a-d), thus triggering a modification of LC3-II/ p62(SQSTM1) ratio in NSC-34 motor neurons (Fig. 2F, a-d).

3.2. *Clomipramine (CMI) and chlorpromazine (CPZ) modulated basal autophagy via lysosomal TPC2 stimulation in NSC-34 motor neuronal cells*

In order to verify the putative regulation exerted by the lysosomal channel on basal autophagy, we tested the effect of CPZ on the expression of some autophagy initiators. The addition of the drug for 1 h induced the phosphorylation of ULK (p-ULK) and AMP-activated protein kinase α (p-AMPK α) (Fig. 3A, a-d), that are considered as specific activators of the cleansing process through the inactivation of mTOR complex-1. Furthermore, CPZ significantly reduced p62/SQSTM1 (Fig. 3B, a-b), while it increased LC3-II expression in NSC-34 motor neurons (Fig. 3C, a-c). Considering the protective effect of autophagy in the neurodegenerative process induced by L-BMAA [16], the effect of CPZ was tested in L-BMAA-treated motor neurons, a model in which the neurotoxin impairs the autophagic flux by reducing the lysosomal channel TRPML1 [16]. The preincubation of NSC-34 motor neurons with CPZ for 1 h prevented L-BMAA-induced mitochondrial suffering at concentrations of 20 μM and 40 μM (Fig. 3D). At the highest concentration (i.e. 80 μM) CPZ induced basal mitochondrial toxicity (Fig. 3D). Of note, the protective effect of CPZ was partially reduced in motor neurons previously silenced for TPC2 (siTPC2, Fig. 3E), thus highlighting a significant role of the lysosomal channel in the neuroprotective action of the drug. As proof of concept, motor neuronal cells were exposed to the endogenous modulator of TPC2, NAADP, preincubated under the same experimental conditions. Of note, preincubation for 1 h with the cell permeable form of NAADP, NAADP-AM, induced a protective effect in NSC-34 cells exposed to L-BMAA that was counteracted by knocking-down the channel with siRNA strategy (Fig. 3E).

Furthermore, we investigated the effect of CMI under the same conditions of CPZ. Interestingly, this drug mimicked the same effects of CPZ. Indeed, after 1 h, CMI: (*i*) induced the phosphorylation of ULK (p-ULK) and AMP-activated protein kinase α (p-AMPK α) (Fig. 4A, a-e), (*ii*) significantly reduced p62/SQSTM1 (Fig. 4B, a-b) and (*iii*) increased LC3-II expression (Fig. 4B, c-e). Once again, modulating TPC2, CMI prevented the reduction of mitochondrial activity by L-BMAA (Fig. 4C), as demonstrated by the ability of siTPC2 to partially prevent the neuroprotection induced by drug preincubation (Fig. 4D). Of note, the neuroprotective effect of CMI and CPZ continued also in NSC-34 motor neurons exposed for 48 h to L-BMAA + rotenone, a specific inhibitor of the mitochondrial respiratory chain complex I, a more detrimental model of neurodegeneration (data not shown).

3.3. *Clomipramine (CMI) and chlorpromazine (CPZ) reverted autophagy and mitochondrial dysfunctions induced by L-BMAA exposure*

Considering the effect of CPZ and CMI on TPC2 activity, their impact on autophagy dysfunction induced by L-BMAA has been investigated more deeply. Of note, the neurotoxin significantly reduced TPC2 protein expression (Fig. 5A, a,b) but not that of LAMP1 (Fig. 5B, a,b) Still,

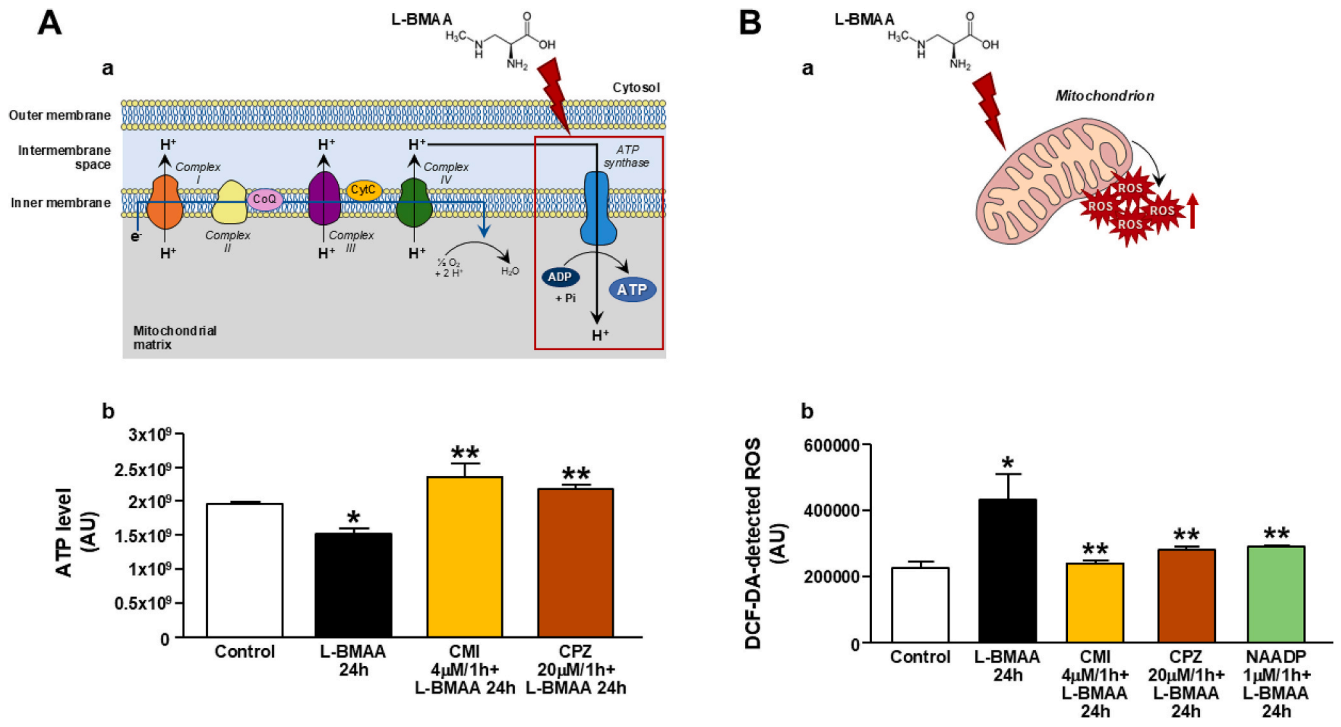

Fig. 7. Clomipramine and chlorpromazine prevented ATP level reduction and ROS overproduction in L-BMAA-treated NSC-34 motor neurons. (A) Representative cartoon depicting the putative interference of L-BMAA with mitochondrial chain and ATP synthesis (a). Intracellular ATP level measurement in NSC-34 cells treated with L-BMAA (300 μM/24 h) and previously incubated with CMI (4 μM/1h) or CPZ (20 μM/1h) (b). Data are expressed as mean ± S.E.M. of three different experimental sessions. *$p < 0.05$ vs control; ** $p < 0.05$ vs L-BMAA 24 h. (B) Representative cartoon illustrating the detrimental effect of L-BMAA on reactive oxygen species (ROS) production at mitochondrial level (a). ROS level quantification in NSC-34 cells treated with L-BMAA (300 μM/24 h) and previously incubated with CMI (4 μM/1h), CPZ (20 μM/1h) or NAADP (1 μM/1h) (b). Data are expressed as mean ± S.E.M. of three different experimental sessions. *$p < 0.05$ vs control; ** $p < 0.05$ vs L-BMAA 24 h.

determining p62 and LC3-II overexpression, L-BMAA produces a blockade of the process [40]. Moreover, preincubation of CPZ or CMI for 1 h counteracted the overexpression of p62 but not of LC3-II protein expression, indicating a significant induction of the autophagic flux (Fig. 5C-D). In this respect, the L-BMAA-induced overexpression of both p62 and LC3-II was further increased by the V-ATPase inhibitor bafilomycin A1 thus indicating a defective but not disrupted autophagic flux (Fig. 5C-D).

Moreover, in motor neuronal cells preincubated with CPZ or CMI for 1 h, deprived of each drug for the following 8 h by washout and, then, exposed to L-BMAA for the remaining 48 h, they counteracted L-BMAA-induced overexpression of both p62 and LC3-II (Fig. 6A-D). This may suggest a restoration of autophagy process to the resting activity.

To investigate the contribution of mitochondria to this phenomenon, the effect of each drug on ATP and ROS production was explored in NSC-34 motor neuronal cells exposed to L-BMAA. In this respect, while the neurotoxin reduced ATP level and triggered ROS overproduction in NSC-34 cells, CPZ and CMI −when preincubated for 1 h before the addition of L-BMAA for the remaining 24 h- significantly prevented these two detrimental effects due to mitochondrial dysfunction, (Fig. 7A, B). As a consequence, for a longer exposure to the toxin, CPZ and CMI significantly counteracted LDH, cytochrome *C* and SMAC/DIABLO release from NSC-34 motor neurons exposed to L-BMAA for 48 h (Fig. 8A,B,C, respectively).

4. Discussion

In consideration of the role of the lysosomal channels in the modulation of autophagy, in this study we showed that the tricyclic antidepressant CMI and the antipsychotic CPZ were capable of effectively stimulating the cationic channel TPC2 in motor neurons thus triggering a protective autophagy in an *in vitro* model of neurodegeneration. This is in accordance with previous studies showing a certain activity of the two drugs at the level of TPC2 in non-neuronal cells [25]. In virtue of this mechanism, CMI and CPZ reduced cell death rate by limiting mitochondrial damage in motor neuronal cells exposed to the neurotoxin L-BMAA, a widely recognized model of ALS/PDC [16,31,41,42].

The protective effects of the two neurological drugs were mimicked by NAADP, a lysosomal second messenger activating TPC2 as unique endogenous modulator. In fact, NAADP specifically induced TPC2-mediated current, triggered nuclear translocation of TFEB, and prevented mitochondrial suffering in motor neuronal cells exposed to L-BMAA. Of note, the protective role of this metabolite has been recently highlighted by the clinical trials on a molecular entity able to modify its concentration through the inhibition of the relative metabolic enzyme SARM1 [43,44]. In this regard, a new disease modifying drug inhibiting SARM1 has entered clinical trials since the expression of its constitutively hyperactivated form has been reported in ALS patients carrying strong gain-of-function variants of the enzyme [43,44]. Furthermore, SARM1 not only has a NADase activity but also catalyzes a base exchange reaction between nicotinic acid and $NADP^+$ to generate NAADP [45]. It has been established that rare *sarm1* alleles encoding variants with constitutive NADase activity are associated with NAD^+ and $NADP^+$ profound reduction in ALS and other motor nerve disorders [43]. Furthermore, SARM1 is also involved in axon degeneration, catalyzing multiple complex mechanisms [45,46]. This evidence highlighted the relevance of NAADP in ALS pathophysiology thus rendering its endogenous receptor/channel (i.e. TPC2) an interesting druggable target. Of note, the mimetic agonist of NAADP on TPC2, TPC2-A1-N [27], perfectly mirrored its mechanism of action by eliciting TPC2-mediated currents, moving lysosomal Ca^{2+}, inducing TFEB nuclear translocation and boosting autophagy in motor neuronal cells.

Another aspect that deserves attention is the modulating ability in triggering autophagy by CMI and CPZ. Becoming dysfunctional during

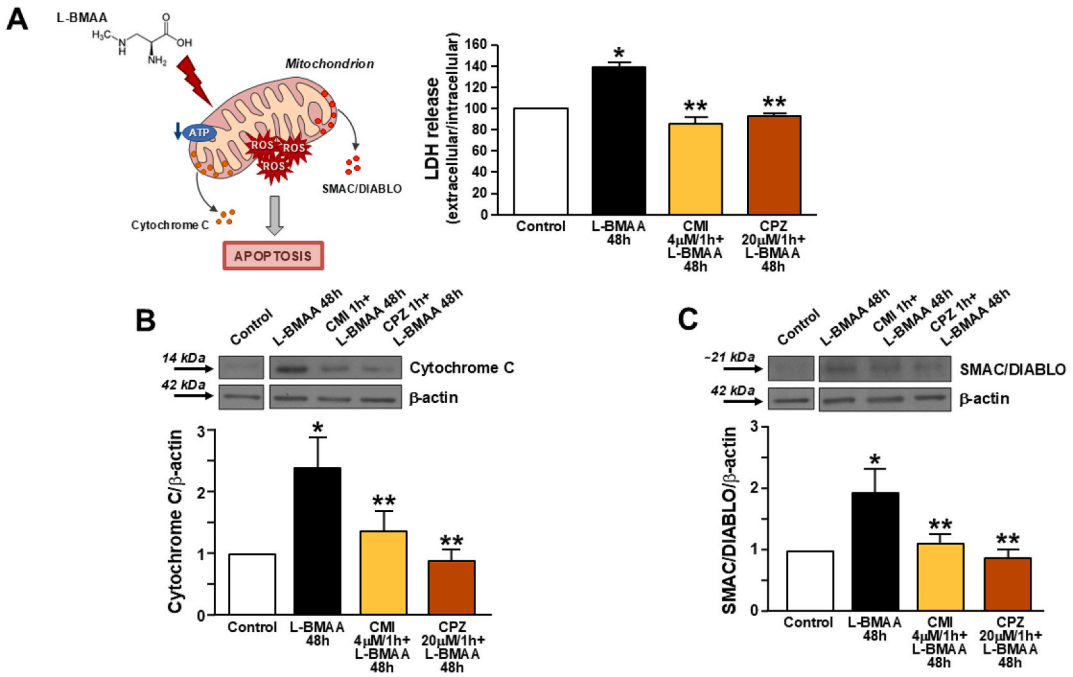

Fig. 8. Clomipramine and chlorpromazine prevented the release of LDH, cytochrome *C* and SMAC/DIABLO in L-BMAA-treated NSC-34 motor neurons. (A) Left: cartoon depicting the release of cytochrome *C* and SMAC/DIABLO from mitochondria induced by L-BMAA. Right: Lactate dehydrogenase (LDH) release measurement in NSC-34 cells treated with L-BMAA (300 μM/48 h) and previously incubated with CMI (4 μM/1h) or CPZ (20 μM/1h). Data are expressed as mean ± S.E.M. of three different experimental sessions. *p < 0.05 vs control; ** p < 0.05 vs L-BMAA 48 h. (B) Representative Western blotting (top) and quantification (bottom) of cytochrome *C* release in motor neurons pretreated with CMI (4 μM) or CPZ (20 μM) 1 h before L-BMAA administration (300 μM/48 h). Data are expressed as mean ± S.E.M. of three different experimental sessions. *p < 0.05 vs control; ** p < 0.05 vs L-BMAA 48 h. (C) Representative Western blotting (top) and quantification (bottom) of SMAC/DIABLO release in motor neurons pretreated with CMI (4 μM) or CPZ (20 μM) 1 h before L-BMAA administration (300 μM/48 h). Data are expressed as mean ± S.E.M. of three different experimental sessions. *p < 0.05 vs control; ** p < 0.05 vs L-BMAA 48 h. Cytochrome *C* and SMAC/DIABLO release was assessed in cytosolic lysates from NSC-34 cells (see Materials and methods section).

ALS progression, autophagy stasis determines the accumulation of detrimental aggregates in suffering motor neurons [12]. This peculiar pathomechanism (e.g. the blockade of autophagy) is shared by several neurodegenerative diseases including Alzheimer's, Huntington's and Parkinson's diseases, as well as several Lysosomal Storage Diseases, thus highlighting the relevance of autophagy dysfunction as new druggable mechanism. For instance, safe autophagy inducers have been identified for the treatment of Huntington's disease [47]. Therefore, in our opinion, each autophagy-activating drug could be considered as a good candidate in ALS therapy. In line with this hypothesis, several new molecular entities modulating autophagy are now screened in ongoing clinical trials on ALS and other neurodegenerative diseases. For instance, a multicenter, randomized, double-blind trial with parental administration of RAPA-501 T cell therapy is running in ALS patients (NCT04220190). RAPA-501 cells are manufactured *ex vivo* by the autophagy inducer rapamycin in order to yield a T cell population with a dual anti-inflammatory phenotype. Previous treatment of patients with rapamycin alone −in a multicenter, randomized, double-blind trial [48]- induced frequent adverse events including skin and gastrointestinal disorders [49]. Moreover, the alternative mTOR pathway inhibitor monepantel is currently screened under phase I trial (NCT04894240) [50].

The present data confirmed the concept that boosting autophagy may be a useful strategy to protect ALS motor neurons. In fact, they highlighted TPC2 stimulation as a new modality to trigger autophagy under physiological and pathological conditions. Furthermore, they suggested that drug repurposing is a useful pharmacological strategy to find new treatments for ALS therapy.

Collectively, given the correlation between autophagy dysregulation and lysosomal malfunction, both associated with ALS progression, this study highlights that CPZ and CMI modulating TPC2 could be useful to draw future treatments and new directions in ALS therapy.

4.1. Conclusions

The present study showed that, at least *in vitro*, CMI and CPZ can activate protective autophagy through lysosomal TPC2 channel activation, thus partially saving motor neurons exposed to the neurotoxic action of L-BMAA, an experimental model of ALS/PDC. The identification of these two drugs occurred through the repurposing strategy that have numerous pharmacological advantages, including the precise picture of the clinical toxicity of the drugs. Certainly, a limitation of this study is that of not having tested *in vivo* these selected drugs. Therefore, further studies on murine models of ALS will be able to confirm the efficacy of the drugs and establish a dosage regimen useful as a starting point for clinical studies. Another limitation of the present study is that the potency of both these ligands against TPC2 is poor, thus rendering necessary to identify other TPC2 activators starting from their chemical structures.

Of note, it is also possible that the broader poly-pharmacology of these drugs could likely determine other pleiotropic effects on the endolysosomal compartment beyond the autophagy modulation.

Funding sources

This research was funded by PRIN (PROGETTI DI RICERCA DI RILEVANTE INTERESSE NAZIONALE) Bando PRIN-PNRR 2022 Prot. P2022P88K5 to A.S., PRIN 2022 Prot. 2022ZTKFXS to A.P. and National Recovery and Resilience Plan (NRRP), project MNESYS (PE0000006).

CRediT authorship contribution statement

Valentina Tedeschi: Methodology, Investigation, Formal analysis, Data curation, Conceptualization. **Raffaella Ciancio:** Methodology, Formal analysis, Data curation. **Giorgia Magliocca:** Methodology. **Emilia Esposito:** Methodology. **Silvia Piccirillo:** Methodology. **Valentina Rubino:** Methodology, Investigation. **Alessandra Preziuso:** Investigation. **Tatiana Spadoni:** Investigation. **Noemi Di Muraglia:** Methodology. **Giuseppina Ruggiero:** Investigation, Formal analysis. **Anna Pannaccione:** Writing – original draft, Methodology, Formal analysis. **Agnese Secondo:** Writing – review & editing, Writing – original draft, Supervision, Resources, Methodology, Investigation, Funding acquisition, Conceptualization.

Declaration of competing interest

The authors declare that they have no known competing financial interests or personal relationships that could have appeared to influence the work reported in this paper.

Acknowledgements

We thank Professor Neil Cashman for the kind gift of NSC-34 cells.

Data availability

Data will be made available on request.

References

[1] P.A. Cox, S.A. Banack, S.J. Murch, Biomagnification of cyanobacterial neurotoxins and neurodegenerative disease among the Chamorro people of Guam, Proc. Natl. Acad. Sci. U. S. A. 100 (2003) 13380–13383, https://doi.org/10.1073/pnas.2235808100.

[2] J. Pablo, S.A. Banack, P.A. Cox, T.E. Johnson, S. Papapetropoulos, W.G. Bradley, A. Buck, D.C. Mash, Cyanobacterial neurotoxin BMAA in ALS and Alzheimer's disease, Acta Neurol. Scand. 120 (2009) 216–225, https://doi.org/10.1111/j.1600-0404.2008.01150.x.

[3] S.M. Corsello, J.A. Bittker, Z. Liu, J. Gould, P. McCarren, J.E. Hirschman, S. E. Johnston, A. Vrcic, B. Wong, M. Khan, J. Asiedu, R. Narayan, C.C. Mader, A. Subramanian, T.R. Golub, The Drug Repurposing Hub: a next-generation drug library and information resource, Nat. Med. 23 (2017) 405–408, https://doi.org/10.1038/nm.4306.

[4] F.A. Badria, Drug Repurposing - Hypothesis, Molecular Aspects and Therapeutic Applications. IntechOpen, London, UK, 2020.

[5] H.A.M. Mucke, Drug Repurposing: then, now, and in the Future, Drug Repurposing 1 (2024) 1–3, https://doi.org/10.58647/DRUGREPO.24.1.0003.

[6] V.S. Kulkarni, V. Alagarsamy, V.R. Solomon, P.A. Jose, S. Murugesan, Drug Repurposing: an Effective Tool in Modern Drug Discovery, Russ. J. Bioorg. Chem. 49 (2023) 157–166, https://doi.org/10.1134/S1068162023020139.

[7] S. Patergnani, M. Bonora, S. Ingusci, M. Previati, S. Marchi, S. Zucchini, M. Perrone, M.R. Wieckowski, M. Castellazzi, M. Pugliatti, C. Giorgi, M. Simonato, P. Pinton, Antipsychotic drugs counteract autophagy and mitophagy in multiple sclerosis, Proc. Natl. Acad. Sci. U. S. A. 118 (2021) e2020078118, https://doi.org/10.1073/pnas.2020078118.

[8] H. Wang, H. Xu, J. Niu, F. Mei, X. Li, J. Kong, W. Cai, L. Xiao, Haloperidol activates quiescent oligodendroglia precursor cells in the adult mouse brain, Schizophr. Res. 119 (2010) 164–174, https://doi.org/10.1016/j.schres.2010.02.1068.

[9] L.K. Green, P. Zareie, N. Templeton, R.A. Keyzers, B. Connor, A.C. La Flamme, Enhanced disease reduction using clozapine, an atypical antipsychotic agent, and glatiramer acetate combination therapy in experimental autoimmune encephalomyelitis, Mult Scler J Exp Transl Clin 3 (2017) 2055217317698724, https://doi.org/10.1177/2055217317698724.

[10] D. O'Sullivan, L. Green, S. Stone, P. Zareie, M. Kharkrang, D. Fong, B. Connor, A. C. La Flamme, Treatment with the antipsychotic agent, risperidone, reduces disease severity in experimental autoimmune encephalomyelitis, PLoS One 9 (2014) e104430, https://doi.org/10.1371/journal.pone.0104430.

[11] L. Xiao, H. Xu, Y. Zhang, Z. Wei, J. He, W. Jiang, X. Li, L.E. Dyck, R.M. Devon, Y. Deng, X.M. Li, Quetiapine facilitates oligodendrocyte development and prevents mice from myelin breakdown and behavioral changes, Mol. Psychiatry 13 (2008) 697–708, https://doi.org/10.1038/sj.mp.4002064.

[12] V. Tedeschi, S. Sapienza, R. Ciancio, L.M.T. Canzoniero, A. Pannaccione, A. Secondo, Lysosomal Channels as New Molecular Targets in the Pharmacological Therapy of Neurodegenerative Diseases via Autophagy Regulation, Curr. Neuropharmacol. (2024), https://doi.org/10.2174/1570159X22666240517101846.

[13] A.R. Winslow, C.W. Chen, S. Corrochano, A. Acevedo-Arozena, D.E. Gordon, A. A. Peden, M. Lichtenberg, F.M. Menzies, B. Ravikumar, S. Imarisio, S. Brown, C. J. O'Kane, D.C. Rubinsztein, α-Synuclein impairs macroautophagy: implications for Parkinson's disease, J. Cell Biol. 190 (2010) 1023–1037, https://doi.org/10.1083/jcb.201003122.

[14] J.H. Lee, W.H. Yu, A. Kumar, S. Lee, P.S. Mohan, C.M. Peterhoff, D.M. Wolfe, M. Martinez-Vicente, A.C. Massey, G. Sovak, Y. Uchiyama, D. Westaway, A. M. Cuervo, R.A. Nixon, Lysosomal proteolysis and autophagy require presenilin 1 and are disrupted by Alzheimer-related PS1 mutations, Cell 141 (2010) 1146–1158, https://doi.org/10.1016/j.cell.2010.05.008.

[15] B. Ravikumar, C. Vacher, Z. Berger, J.E. Davies, S. Luo, L.G. Oroz, F. Scaravilli, D. F. Easton, R. Duden, C.J. O'Kane, D.C. Rubinsztein, Inhibition of mTOR induces autophagy and reduces toxicity of polyglutamine expansions in fly and mouse models of Huntington disease, Nat. Genet. 36 (2004) 585–595, https://doi.org/10.1038/ng1362.

[16] V. Tedeschi, T. Petrozziello, M.J. Sisalli, F. Boscia, L.M.T. Canzoniero, A. Secondo, The activation of Mucolipin TRP channel 1 (TRPML1) protects motor neurons from L-BMAA neurotoxicity by promoting autophagic clearance, Sci. Rep. 9 (2019) 10743, https://doi.org/10.1038/s41598-019-46708-5.

[17] V. Tedeschi, V. Nele, V. Valsecchi, S. Anzilotti, A. Vinciguerra, L. Zucaro, M. J. Sisalli, C. Cassiano, N. De Iesu, G. Pignataro, L.M.T. Canzoniero, A. Pannaccione, G. De Rosa, A. Secondo, Nanoparticles encapsulating phosphatidylinositol derivatives promote neuroprotection and functional improvement in preclinical models of ALS via a long-lasting activation of TRPML1 lysosomal channel, Pharmacol. Res. 210 (2024) 107491, https://doi.org/10.1016/j.phrs.2024.107491.

[18] V. Tedeschi, A. Vinciguerra, M.J. Sisalli, G. Pignataro, A. Secondo, Pharmacological inhibition of lysosomal two-pore channel 2 (TPC2) confers neuroprotection in stroke via autophagy regulation, Neurobiol. Dis. 178 (2023) 106020, https://doi.org/10.1016/j.nbd.2023.106020.

[19] X.S. Wang, Z. Tian, N. Zhang, J. Han, H.L. Guo, M.G. Zhao, S.B. Liu, Protective Effects of Gastrodin against Autophagy-Mediated Astrocyte Death, Phytother. Res. 30 (2016) 386–396, https://doi.org/10.1002/ptr.5538.

[20] J. Belgrad, R. De Pace, R.D. Fields, Autophagy in Myelinating Glia, J. Neurosci. 40 (2020) 256–266, https://doi.org/10.1523/JNEUROSCI.1066-19.2019.

[21] D.C. Rubinsztein, J.E. Gestwicki, L.O. Murphy, D.J. Klionsky, Potential therapeutic applications of autophagy, Nat. Rev. Drug Discov. 6 (2007) 304–312, https://doi.org/10.1038/nrd2272.

[22] D.L. Medina, S. Di Paola, I. Peluso, A. Armani, D. De Stefani, R. Venditti, S. Montefusco, A. Scotto-Rosato, C. Prezioso, A. Forrester, C. Settembre, W. Wang, Q. Gao, H. Xu, M. Sandri, R. Rizzuto, M.A. De Matteis, A. Ballabio, Lysosomal calcium signalling regulates autophagy through calcineurin and TFEB, Nat. Cell Biol. 17 (2015) 288–299, https://doi.org/10.1038/ncb3114.

[23] G.J. Pereira, H. Hirata, G.M. Fimia, do Carmo L.G., Bincoletto C., Han S.W., Stilhano R.S., Ureshino R.P., Bloor-Young D., Churchill G., Piacentini M., Patel S., Smaili S.S., Nicotinic acid adenine dinucleotide phosphate (NAADP) regulates autophagy in cultured astrocytes, J. Biol. Chem. 286 (2011) 27875, https://doi.org/10.1074/jbc.C110.216580.

[24] A. Galione, A primer of NAADP-mediated Ca(2+) signalling: from sea urchin eggs to mammalian cells, Cell Calcium 58 (2015) 27–47, https://doi.org/10.1016/j.ceca.2014.09.010.

[25] X. Zhang, W. Chen, P. Li, R. Calvo, N. Southall, X. Hu, M. Bryant-Genevier, X. Feng, Q. Geng, C. Gao, M. Yang, K. Tang, M. Ferrer, J.J. Marugan, H. Xu, Agonist-specific voltage-dependent gating of lysosomal two-pore Na^+ channels, Elife 8 (2019) e51423, https://doi.org/10.7554/eLife.51423.

[26] M. Schieder, K. Rötzer, A. Brüggemann, M. Biel, C.A. Wahl-Schott, Characterization of two-pore channel 2 (TPCN2)-mediated Ca^{2+} currents in isolated lysosomes, J. Biol. Chem. 285 (2010) 21219–21222, https://doi.org/10.1074/jbc.C110.143123.

[27] Gerndt S., Chen C.C., Chao Y.K., Yuan Y., Burgstaller S., Scotto Rosato A., Krogsaeter E., Urban N., Jacob K., Nguyen O.N.P., Miller M.T., Keller M., Vollmar A.M., Gudermann T., Zierler S., Schredelseker J., Schaefer M., Biel M., Malli R., Wahl-Schott C., Bracher F., Patel S., Grimm C. Agonist-mediated switching of ion selectivity in TPC2 differentially promotes lysosomal function. *Elife*, 2020; 9: e54712. doi: 10.7554/eLife.54712.

[28] R.A. Scotto, E.K. Krogsaeter, D. Jaślan, C. Abrahamian, S. Montefusco, C. Soldati, B. Spix, M.T. Pizzo, G. Grieco, J. Böck, A. Wyatt, D. Wünkhaus, M. Passon, M. Stieglitz, M. Keller, G. Hermey, S. Markmann, D. Gruber-Schoffnegger, S. Cotman, L. Johannes, D. Crusius, U. Boehm, C. Wahl-Schott, M. Biel, F. Bracher, E. De Leonibus, E. Polishchuk, D.L. Medina, D. Paquet, C. Grimm, TPC2 rescues lysosomal storage in mucolipidosis type IV, Niemann-pick type C1, and Batten disease, EMBO Mol. Med. 14 (2022) e15377, https://doi.org/10.15252/emmm.202115377.

[29] N.R. Nabar, C.N. Heijjer, C.S. Shi, I.Y. Hwang, S. Ganesan, M.C.I. Karlsson, J. H. Kehrl, LRRK2 is required for CD38-mediated NAADP-Ca^{2+} signaling and the downstream activation of TFEB (transcription factor EB) in immune cells, Autophagy 18 (2022) 204–222, https://doi.org/10.1080/15548627.2021.1954779.

[30] N.R. Cashman, H.D. Durham, J.K. Blusztajn, K. Oda, T. Tabira, I.T. Shaw, S. Dahrouge, J.P. Antel, Neuroblastoma x spinal cord (NSC) hybrid cell lines resemble developing motor neurons, Dev. Dyn. 194 (1992) 209–221, https://doi.org/10.1002/aja.1001940306.

[31] T. Petrozziello, A. Secondo, V. Tedeschi, A. Esposito, M. Sisalli, A. Scorziello, G. Di Renzo, L. Annunziato, ApoSOD1 lacking dismutase activity neuroprotects motor neurons exposed to beta-methylamino-L-alanine through the Ca^{2+}/Akt/ERK1/2

prosurvival pathway, Cell Death Differ. 24 (2017) 511–522, https://doi.org/10.1038/cdd.2016.154.
[32] X. Wang, X. Zhang, X.P. Dong, M. Samie, X. Li, X. Cheng, A. Goschka, D. Shen, Y. Zhou, J. Harlow, M.X. Zhu, D.E. Clapham, D. Ren, H. Xu, TPC proteins are phosphoinositide- activated sodium-selective ion channels in endosomes and lysosomes, Cell 151 (2012) 372–383, https://doi.org/10.1016/j.cell.2012.08.036.
[33] X.P. Dong, D. Shen, X. Wang, T. Dawson, X. Li, Q. Zhang, X. Cheng, Y. Zhang, L. S. Weisman, M. Delling, H. Xu, PI(3,5)P(2) controls membrane trafficking by direct activation of mucolipin Ca(2+) release channels in the endolysosome, Nat. Commun. 1 (2010) 38, https://doi.org/10.1038/ncomms1037.
[34] X.Z. Zhong, X.P. Dong, Lysosome electrophysiology, Methods Cell Biol. 126 (2015) 197–215, https://doi.org/10.1016/bs.mcb.2014.10.022.
[35] X. Zhang, W. Chen, Q. Gao, J. Yang, X. Yan, H. Zhao, L. Su, M. Yang, C. Gao, Y. Yao, K. Inoki, D. Li, R. Shao, S. Wang, N. Sahoo, F. Kudo, T. Eguchi, B. Ruan, H. Xu, Rapamycin directly activates lysosomal mucolipin TRP channels independent of mTOR, PLoS Biol. 17 (2019) e3000252, https://doi.org/10.1371/journal.pbio.3000252.
[36] J.J. Dougherty, J. Wu, R.A. Nichols, Beta-amyloid regulation of presynaptic nicotinic receptors in rat hippocampus and neocortex, J. Neurosci. 23 (2003) 6740–6747, https://doi.org/10.1523/JNEUROSCI.23-17-06740.2003.
[37] A. Secondo, R.I. Staiano, A. Scorziello, R. Sirabella, F. Boscia, A. Adornetto, V. Valsecchi, P. Molinaro, L.M. Canzoniero, G. Di Renzo, L. Annunziato, BHK cells transfected with NCX3 are more resistant to hypoxia followed by reoxygenation than those transfected with NCX1 and NCX2: possible relationship with mitochondrial membrane potential, Cell Calcium 42 (2007) 521–535, https://doi.org/10.1016/j.ceca.2007.01.006.
[38] G. Magliocca, E. Esposito, M. Tufano, I. Piccialli, V. Rubino, V. Tedeschi, M. J. Sisalli, F. Carriero, G. Ruggiero, A. Secondo, L. Annunziato, A. Scorziello, A. Pannaccione, Involvement of $K_V3.4$ Channel in Parkinson's Disease: a Key Player in the Control of Midbrain and Striatum Differential Vulnerability during Disease Progression? Antioxidants (basel) 13 (2024) 999, https://doi.org/10.3390/antiox13080999.
[39] G. Terrazzano, S. Bruzzaniti, V. Rubino, M. Santopaolo, A.T. Palatucci, A. Giovazzino, C. La Rocca, P. de Candia, A. Puca, F. Perna, C. Procaccini, V. De Rosa, C. Porcellini, S. De Simone, V. Fattorusso, A. Porcellini, E. Mozzillo, R. Troncone, A. Franzese, J. Ludvigsson, G. Matarese, G. Ruggiero, M. Galgani, T1D progression is associated with loss of $CD3^+CD56^+$ regulatory T cells that control $CD8^+$ T cell effector functions, Nat Metab 2 (2020) 142–152, https://doi.org/10.1038/s42255-020-0173-1.
[40] K. Wang, Q. Gong, Y. Zhan, B. Chen, T. Yin, Y. Lu, Y. Zhang, H. Wang, J. Ke, B. Du, X. Liu, J. Xiao, Blockage of Autophagic Flux and Induction of Mitochondria Fragmentation by Paroxetine Hydrochloride in Lung Cancer Cells Promotes Apoptosis via the ROS-MAPK Pathway, Front. Cell Dev. Biol. 7 (2020) 397, https://doi.org/10.3389/fcell.2019.00397.
[41] S.D. Rao, S.A. Banack, P.A. Cox, J.H. Weiss, BMAA selectively injures motor neurons via AMPA/kainate receptor activation, Exp. Neurol. 201 (2006) 244–252, https://doi.org/10.1016/j.expneurol.2006.04.017.
[42] Beri J., Nash T., Martin R.M., Bereman M.S. Exposure to BMAA mirrors molecular processes linked to neurodegenerative disease. *Proteomics*, 2017; 17:10.1002/pmic.201700161. doi: 10.1002/pmic.201700161.
[43] Gilley J., Jackson O., Pipis M., Estiar M.A., Al-Chalabi A., Danzi M.C., van Eijk K.R., Goutman S.A., Harms M.B., Houlden H., Iacoangeli A., Kaye J., Lima L.; Queen Square Genomics; Ravits J., Rouleau G.A., Schüle R., Xu J., Züchner S., Cooper-Knock J., Gan-Or Z., Reilly M.M., Coleman M.P. Enrichment of *SARM1* alleles encoding variants with constitutively hyperactive NADase in patients with ALS and other motor nerve disorders. *Elife*, 2021; 10:e70905. doi: 10.7554/eLife.70905.
[44] A.J. Bloom, X. Mao, A. Strickland, Y. Sasaki, J. Milbrandt, A. DiAntonio, Constitutively active SARM1 variants that induce neuropathy are enriched in ALS patients, Mol. Neurodegener. 17 (2022) 1, https://doi.org/10.1186/s13024-021-00511-x.
[45] J.D. Icso, L. Barasa, P.R. Thompson, SARM1, an Enzyme involved in Axon Degeneration, Catalyzes Multiple Activities through a Ternary complex Mechanism, Biochemistry 62 (2023) 2065–2078, https://doi.org/10.1021/acs.biochem.3c00081.
[46] C. Angeletti, A. Amici, J. Gilley, A. Loreto, A.G. Trapanotto, C. Antoniou, E. Merlini, M.P. Coleman, G. Orsomando, SARM1 is a multi-functional NAD(P)ase with prominent base exchange activity, all regulated bymultiple physiologically relevant NAD metabolites, iScience 25 (2022) 103812, https://doi.org/10.1016/j.isci.2022.103812.
[47] B.R. Underwood, Z.W. Green-Thompson, P.J. Pugh, S.E. Lazic, S.L. Mason, J. Griffin, P.S. Jones, J.B. Rowe, D.C. Rubinsztein, R.A. Barker, An open-label study to assess the feasibility and tolerability of rilmenidine for the treatment of Huntington's disease, J. Neurol. 264 (2017) 2457–2463, https://doi.org/10.1007/s00415-017-8647-0.
[48] J. Mandrioli, R. D'Amico, E. Zucchi, S. De Biasi, F. Banchelli, I. Martinelli, C. Simonini, T.D. Lo, R. Vicini, N. Fini, G. Gianferrari, M. Pinti, C. Lunetta, F. Gerardi, C. Tarlarini, L. Mazzini, F. De Marchi, A. Scognamiglio, G. Sorarù, A. Fortuna, G. Lauria, E.D. Bella, C. Caponnetto, G. Meo, A. Chio, A. Calvo, A. Cossarizza, Randomized, double-blind, placebo-controlled trial of rapamycin in amyotrophic lateral sclerosis, Nat. Commun. 14 (2023) 4970, https://doi.org/10.1038/s41467-023-40734-8.
[49] X. Li, R. Bedlack, Evaluating emerging drugs in phase II & III for the treatment of amyotrophic lateral sclerosis, Expert Opin. Emerg. Drugs 29 (2024) 93–102, https://doi.org/10.1080/14728214.2024.2333420.
[50] E. Angelopoulou, E.S. Pyrgelis, C. Piperi, Emerging potential of the Phosphodiesterase (PDE) Inhibitor Ibudilast for Neurodegenerative Diseases: an Update on Preclinical and Clinical evidence, Molecules 27 (2022) 8448, https://doi.org/10.3390/molecules27238448.